Measurements of Very Low Bit-Error Rates for an Optical Packet Switching Node

Benjamin A. Small, *Student Member, IEEE*, Tatsuya Kato, and Keren Bergman, *Member, IEEE*

***Abstract*—An improvement in the accuracy of the sinusoidal interference method used to extract bit-error rates (BERs) that cannot be easily measured with conventional laboratory equipment is proposed. This technique is then used to estimate the very low BER performance of a multiple-wavelength photonic switching node for a 16-wavelength packet payload. The switching node contribution to the estimated BER is determined to be no worse than 4×10^{-18} from an extrapolated q-factor of 8.6.**

***Index Terms*—Bit-error rate (BER), packet switching, photonic switching systems, wavelength-division multiplexing (WDM).**

I. Introduction

OPTICAL packet switching (OPS) networks maintain payload information in the optical domain in order to support bit-rate and format transparency, improve routing latency, and eliminate the cost and footprint associated with complex optoelectronic and electrooptic conversions [1]–[3]. Switching nodes and routing modules within OPS systems are, therefore, designed to transmit the optically encoded information as transparently as possible: The incoming optical data should match the outgoing optical data as closely as possible, in terms of optical power, optical signal-to-noise ratio, etc.

An elemental broad-band 1×2 switching node has been developed which is designed for multiple-wavelength packets (Fig. 1) [4], [5], and these nodes have been assembled successfully to form a 12×12 routing network [6]. The wavelength-parallel packet format contains a multiple-wavelength payload, and two routing header wavelengths (frame or "F," and address or "A") which are detected by the node in order to make the appropriate routing decision, as executed by enabling one of the two semiconductor optical amplifier (SOA) switching elements [4], [5]. The packet is then self-routed through the switching node while preserving the optical payload. This switching node design demonstrates a high degree of transparency, with a receiver power penalty of 0.2 dB [5].

In this letter, the transparency of the implemented OPS node is demonstrated further by determining an estimated bit-error rate (BER) introduced by the node itself. An improved sinusoidal interference method is introduced and employed as a means of extrapolating low BER levels which are not ordinarily easy to obtain in conventional laboratory experiments. While the BER levels discussed for a single switching node seem extraordinarily low, they are meaningful to the application of petascale supercomputing interconnection networks, which could contain 1000's of OPS nodes and 100's of Tb/s of bisectional bandwidth.

Manuscript received June 1, 2005; revised June 20, 2005. This work was supported in part by the National Science Foundation under Grant ECS-0322813 and in part by the U.S. Department of Defense under Subcontract B-12-644.

The authors are with the Department of Electrical Engineering, Columbia University, New York, NY 10027 USA (e-mail: bas@ee.columbia.edu; tk2136@columbia.edu; bergman@ee.columbia.edu).

Digital Object Identifier 10.1109/LPT.2005.857592

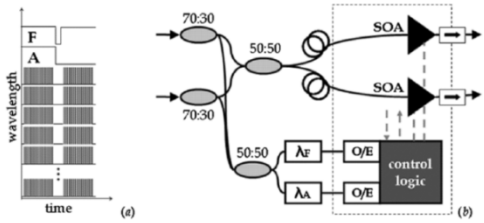

Fig. 1. (a) Illustration of the WDM wavelength-parallel packet format. (b) Schematic of the implemented OPS node (ovals for optical couplers, λ filters, optical-to-electrical (O/E) photodetectors, and boxed arrows for isolators, dashed arrows for deflection signal input and output) [5].

II. Methodology

The sinusoidal interference method has been advocated as an efficient and accurate methodology for extrapolating very low BERs [7]–[9]. The theoretical basis of this technique is the canonical estimation of the BER, assuming a Gaussian noise distribution, given as the probability of error for each bit P_e

$$P_e = \frac{1}{4}\left[\operatorname{erfc}\left(\frac{I_1 - I_{\text{th}}}{\sqrt{2}\sigma_1}\right) + \operatorname{erfc}\left(\frac{I_{\text{th}} - I_0}{\sqrt{2}\sigma_0}\right)\right] \tag{1}$$

where $\operatorname{erfc}(\cdot)$ is the complimentary error function, and $I_{1,0}$ and $\sigma_{1,0}$ are the signal intensities and noise levels of the "1" and "0" bits, respectively, and I_{th} is the decision threshold. The conventional linear q-factor signal-to-noise ratio is

$$q = \frac{I_1 - I_0}{\sigma_1 + \sigma_0} \tag{2}$$

and, thus, the minimum BER can be further approximated by assuming symmetrical noise between "1" and "0" bits

$$P_e(q) = \frac{1}{2}\operatorname{erfc}\left(\frac{q}{\sqrt{2}}\right). \tag{3}$$

However, if a sinusoidal disturbance (interference) with amplitude $A_{\sin}$ is applied to the optimal decision threshold I_{th}, the resulting observed BER estimate is then

$$\hat{P}_e(q - \rho) = \frac{1}{2}\operatorname{erfc}\left(\frac{q - \rho}{\sqrt{2}}\right) \tag{4}$$

where $\rho = A_{\sin}/\sigma_{0,1}$.

Therefore, the unperturbed $(A_{\sin} \to 0)$ minimum BER (3) can be estimated by extrapolation

$$\hat{P}_e(q) = \operatorname*{Lim}_{\rho \to 0} \frac{1}{2}\operatorname{erfc}\left(\frac{q - \rho}{\sqrt{2}}\right). \tag{5}$$

TABLE I
VALUES OF APPROXIMATION CONSTANTS AND RMS ERROR

	Chrostowski [7],[8]	Small
c_0	0.7912	0.8909
c_1	0.2498	0.2360
c_2	0.4926	0.4928
RMS error		
$7 \le q-\rho \le 8$:	0.97 %	0.18 %
$6 \le q-\rho \le 9$:	1.18 %	0.21 %
$5 \le q-\rho \le 12$:	1.26 %	1.11 %

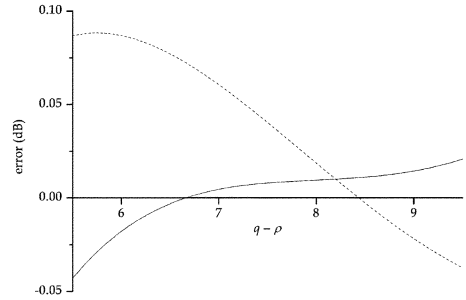

Fig. 2. Plot of the normalized error between the approximation (6) and the exact expression (4), using the constants $c_{0,1,2}$ from Chrostowski [7], [8] (- -) and the authors' constants (—).

This calculation requires an invertible approximation of the transcendental definition of $\hat{P}_e$; a common form is

$$\hat{P}_e(q-\rho) \approx \frac{1}{2}\exp\{-c_2(q-\rho)^2 - c_1(q-\rho) - c_0\} \qquad (6)$$

where $c_{0,1,2}$ are constants. The relevant solution of (6) is

$$q-\rho = \frac{-c_1 + \sqrt{c_1^2 - 4c_2(c_0 + \log|2\hat{P}_e|)}}{2c_2}. \qquad (7)$$

This result is utilized in [7]–[9], but the values given for the constants $c_{0,1,2}$, as given in Table I, may be adjusted. A hypergeometric approximation is given in [10], but this function is difficult to fit into a form similar to (7) for linear regression. Additionally, the values from Chrostowski [7], [8] are not optimal for typical BER levels. In order to minimize the root-mean-square (rms) error between (4) and (6) over the range of q-factor values from 6 to 9 (BER from $\sim 10^{-19}$ to $\sim 10^{-9}$), which are typical for the measurements described below, we present a new set of constants for (7). The constants were obtained from a second-order series expansion of (4) specifically optimized for q-factor values in the range of interest. The values of these constants and the rms errors resulting from using them in (6) compared to (4) are summarized in Table I and plotted in Fig. 2.

Although the improvement in the rms error and the difference in magnitude between the two sets of constants appear small, the sinusoidal interference method often requires extrapolation by almost a factor of five, as shown below and in [7]–[9]. Thus, even small inaccuracies are amplified significantly during the measurement of the estimate $\hat{P}_e$, and the additional accuracy offered by this new approximation is significant (Table I, Fig. 2).

III. EXPERIMENTAL SETUP

This modified methodology is applied in an experimental measurement of the estimated BER contribution from a switching element employed in a multiple-wavelength OPS system. The low BER level (as extrapolated from the q-factor) added by this switching node cannot be directly measured with conventional BER testing equipment.

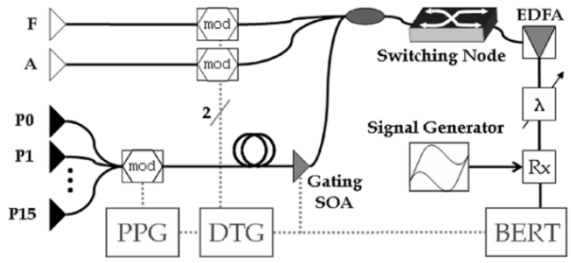

Fig. 3. Schematic of experimental setup with the appropriate packet generation and detection subsystems, with $LiNbO_3$ modulators (mod), pulse pattern generator (PPG), data timing generator (DTG), BER tester (BERT), EDFA amplifier, tunable filter (λ), and p-i-n TIA LA receiver (Rx) with offset provided by the signal generator.

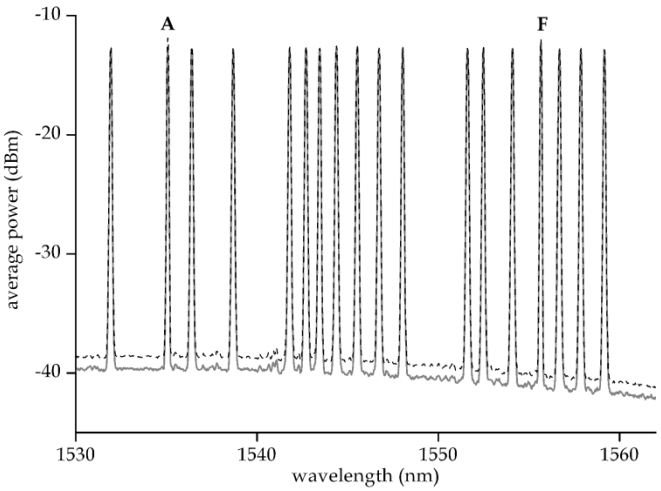

Fig. 4. Plot of input packet optical power spectrum (—) and output packet optical power spectrum (- -) of the 16 payload wavelengths, with the two routing wavelengths annotated.

In order to generate packets of the correct format for the implemented switching node, two routing header wavelengths are required, in addition to the wavelength-parallel optical payload which itself contains 16 wavelengths [4], [5]. These 10-Gb/s NRZ payload wavelengths are modulated together and then decorrelated by approximately 450 ps/nm with 25 km of fiber. The wavelengths used for both the payload and header are channels designated by the ITU wavelength-division-multiplexing (WDM) grid, and some adjacent channels with a spacing of just 0.8 nm (100 GHz) are included. The 16-wavelength payload is then amplified and gated into packets by an SOA. This multiple-wavelength packet payload is coupled with the appropriate wavelength-parallel routing headers, and the whole packet is injected into the switching node (Figs. 3 and 4).

The packet is extracted from the node output and then amplified with an erbium-doped fiber amplifier (EDFA) and filtered for BER testing on one payload wavelength at a time. The BER tester is gated and synchronized to enable error testing only on the packet payload. The p-i-n diode receiver module which contains a transimpedance amplifier (TIA) and a dc-coupled limiting amplifier (LA) for postamplification is perturbed with a

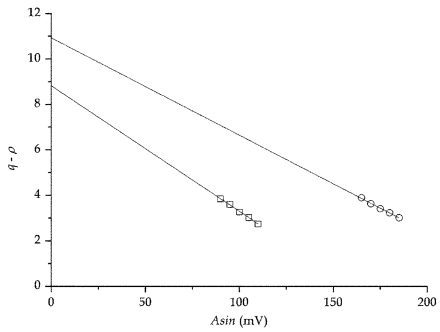

Fig. 5. Plot of q-factor regressions for the back-to-back testbed (○) and for the switching node (□) at the 1554.1-nm (C29) wavelength, as an example of a typical data pair. For the back-to-back extrapolation, $q = 10.93$ ($\hat{P}_e = 4.1 \times 10^{-28}$) with $R^2 = 99.7\%$; and for the switching node, $q = 8.82$ ($\hat{P}_e = 5.4 \times 10^{-19}$) with $R^2 = 99.5\%$.

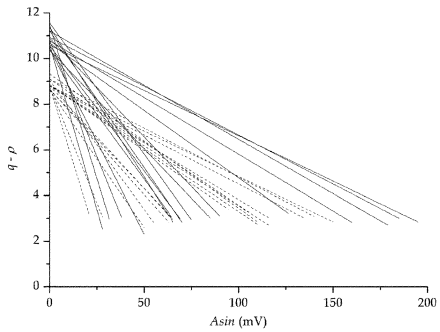

Fig. 6. Plot of q-factor regressions for the back-to-back testbed (—) and for the switching node (- -) for the 16 payload wavelengths.

sinusoidal signal generator at 9 kHz, which is applied to the LA decision threshold within the receiver module.

It is known that the sinusoidal perturbation frequency must be chosen very carefully in order to minimize beating between the perturbation and any of the signals under test [9]. The packet rate for these experiments is approximately 39 MHz, and the pattern repetition rate is 9.7 MHz. However, because a low-pass filter precedes the decision threshold input to the receiver circuitry, a lower frequency sinusoid must be used. It was found that the best and most consistent results are obtained for a 9-kHz sinusoid.

IV. Results

First, in order to confirm the integrity of the optical testbed, back-to-back measurements are performed for the packet generation and detection systems. The intensity of the sinusoidal perturbation is increased as BER measurements are made. Because the sensitivity of the receiver varies slightly between wavelengths, and because of the wavelength dependencies of other components, especially the EDFA, each wavelength responds differently to the same perturbation magnitude $A_{\sin}$. However, the perturbation-free extrapolations are fairly uniform over all payload wavelengths. Moreover, conventional techniques were easily able to obtain error-free measurements on all wavelengths.

All linear regressions are extrapolated from the perturbed BER measurements based on (7) using the least squares method. The regressions are fit with an R^2 correlation coefficient of better than 98% within the sample data for each wavelength (Fig. 5). Five sample data points at differing degrees of perturbation are used for every wavelength. The back-to-back extrapolated q-factor is found to be between 10.4 and 11.5 ($\hat{P}_e$ between 7×10^{-31} and 1×10^{-25}), depending on wavelength; the average q-factor is 10.8, which implies $\hat{P}_e = 2 \times 10^{-27}$ (Fig. 6).

Then, the switching node is inserted into testbed, and the same measurements are recorded and extrapolated. Minimal BER is obtained for packets with a power of approximately −13 dBm per payload wavelength (almost 0-dBm total packet power). The spectra of the incoming and outgoing packets demonstrate the addition of a small amount of ASE noise due to the SOA switching elements (Fig. 4). Again, R^2 for each set of five data points is better than 98%. The extrapolated q-factor for a single pass of the switching node is found to be between 8.6 and 9.3 ($7 \times 10^{-21} \leq \hat{P}_e \leq 4 \times 10^{-18}$) for the 16-wavelength packet payload; with a q-factor of 8.8 ($\hat{P}_e = 7 \times 10^{-19}$) on average (Fig. 6).

Thus, the estimated BER induced by the switching node itself is at most 4×10^{-18}. The back-to-back testbed BER is sufficiently low (better than 1×10^{-25}) that it can be neglected for this measurement.

V. Conclusion

An improvement to the mathematics of the sinusoidal interference method is proposed, and its benefit in terms of numerical accuracy is illustrated. This revised methodology is then applied to a multiple-wavelength OPS node, and the results provide further evidence for the transparency and utility of the implemented switching node design.

References

[1] R. S. Tucker and W. D. Zhong, "Photonic packet switching: An overview," *IEICE Trans. Electron.*, vol. E82-C, pp. 202–212, Feb. 1999.

[2] G. I. Papadimitriou, C. Papazoglou, and A. S. Pomportsis, "Optical switching: Switch fabrics, techniques, and architectures," *J. Lightw. Technol.*, vol. 21, no. 2, pp. 384–405, Feb. 2003.

[3] R. Hemenway, R. R. Grzybowski, C. Minkenberg, and R. Luijten, "Optical-packet-switched interconnect for supercomputer applications," *J. Opt. Networking*, vol. 3, pp. 900–913, Dec. 2004.

[4] A. Shacham, B. A. Small, O. Liboiron-Ladouceur, J. P. Mack, and K. Bergman, "An ultra-low latency routing node for optical packet interconnection networks," in *Proc. 17th Annu. Meeting LEOS*, Nov. 2004, Paper WM2, pp. 565–566.

[5] B. A. Small, A. Shacham, and K. Bergman, "Ultra-low latency optical packet switching node," *IEEE Photon. Technol. Lett.*, vol. 17, no. 7, pp. 1564–1566, Jul. 2005.

[6] B. A. Small, O. Liboiron-Ladouceur, A. Shacham, J. P. Mack, and K. Bergman, "Demonstration of a complete 12-port terabit capacity optical packet switching fabric," in *Proc. Optical Fiber Commun. Conf. (OFC)*, Anaheim, CA, Mar. 2005, Paper OWK1.

[7] P. Palacharla, J. Chrostowski, R. Neumann, and R. J. Gallenberger, "Techniques for accelerated measurement of low bit error rates in computer data links," in *Proc. IEEE 14th Annu. Int. Phoenix Conf. Computers Commun.*, Mar. 1995, pp. 184–190.

[8] J. Zhou, J. Chrostowski, and P. Myslinski, "Measurements of very low bit-error rates of optical switches based on semiconductor optical amplifiers," *IEEE Photon. Technol. Lett.*, vol. 9, no. 8, pp. 1131–1133, Aug. 1997.

[9] X. Wang, F. Kiamilev, P. Gui, J. Ekman, G. C. Papen, M. J. McFadden, M. W. Haney, and C. Kuznia, "A 2-Gb/s optical transceiver with accelerated bit-error-ratio test capability," *J. Lightw. Technol.*, vol. 22, no. 9, pp. 2158–2167, Sep. 2004.

[10] N. S. Bergano, F. W. Kerfoot, and C. R. Davidson, "Margin measurements in optical amplifier systems," *IEEE Photon. Technol. Lett.*, vol. 5, no. 3, pp. 304–306, Mar. 1993.